# Microfabricated Otto chip device for surface plasmon resonance based optical sensing

EDUARDO FONTANA,[1,†,*] JUNG–MU KIM,[2,†] IGNACIO LLAMAS–GARRO,[3] AND GUSTAVO OLIVEIRA CAVALCANTI[4]

[1]*Departamento de Eletrônica e Sistemas, Universidade Federal de Pernambuco, Recife 50740-550, Brazil*
[2]*Division of Electronic Engineering, Chonbuk National University, Jeonju 561-756, Republic of Korea*
[3]*Centre Tecnològic de Telecomunicacions de Catalunya - Castelldefels 08860 , Spain*
[4]*Escola Politécnica, Universidade de Pernambuco - Recife 50720-001, Brazil*

**Corresponding author: fontana@ufpe.br*
*[†]These authors contributed equally to this work*

**Surface plasmon resonance (SPR) based sensors are usually designed using the Kretschnmann prism coupling configuration in which an input beam couples with a surface plasmon through a thin metal film. This is generally preferred by sensor developers for building planar devices instead of the Otto prism coupling configuration, which, for efficient coupling, requires the metal surface to be maintained at a distance on the order of the wavelength from the input prism surface. In this paper we report on the microfabrication and characterization of an Otto chip device, suitable for applications of the SPR effect in gas sensing and biosensing.**

## 1. Introduction

The surface plasmon resonance (SPR) effect observed on metal surfaces [1], thin metal films [2] and metal gratings [3] has been used by researchers in a number of applications, including the characterization of surface roughness [4], measurement of complex refractive index of metals [5], for enhancing interface nonlinearities, as in the surface enhanced Raman scattering [6], to name a few applications. After its identification in the 1980s as a suitable optical transduction mechanism for gas sensing and biosensing [7, 8], it found widespread commercial use for the latter application in the early 1990s, when real-time, label-free, monitoring systems of biomolecular reactions started to reach the market [9,10,11].

For the specific application in biosensing, practical versions of real-time systems based on the SPR effect exploit the Kretschmann configuration [2], as illustrated in Fig.1a, with a metal film thickness of approximately 50 to 60 nm. The exposed metal surface is functionalized with a thin, bioactive, organic layer, having refractive index $n$ and the biological analyte in solution flows through a thin channel (not shown) above the metal surface [10, 11]. The measurement comprises basically detecting refractive index changes in the organic layer due to a biological reaction. For this type of application, the so-called Otto configuration has not been explored. Differently than the Kretschmann configuration, Otto's, illustrated in Fig.1b, requires the metal surface to be separated from the bare glass surface by a gap distance $d_g$ on the order of the wavelength. It is not difficult to set-up the Otto scheme with a gap distance that can be adjusted to enable reaching the critical coupling of the SPR effect, as originally demonstrated by Otto [1], or alternatively with a rigid, transparent, spacer coating on the metal having proper thickness and refractive index to enable observation of the SPR effect. The latter has been demonstrated in the literature, e.g., in the characterization of overcoated aluminum mirrors by SPR [12]. Fabricating a sealed flow channel with an empty gap in the Otto configuration, on the other hand, without offsetting the gap distance for critical coupling, is difficult to achieve and this may probably be the reason why the Otto configuration has not been implemented for practical biosensing devices. Although the sensing performance of an SPR transducer in a waveguide configuration similar to the Otto scheme has been simulated previously [13], no such structure has yet been fabricated with a clear demonstration of the SPR effect.

Use of the Otto configuration could bring a number of benefits in the technology of SPR-based optical sensing. For instance the degrading effect produced by the adhesion layer on the quality factor of the resonance curve, observed in the Kretschmann configuration [9], would not occur in the Otto scheme, given that in the latter, much thicker values of the active layer—in general a high purity gold film — can be employed. Because of this, the adhesion layer does not disturb the evanescent surface plasmon amplitude profile within the active layer. In addition, it is well known that optical losses increase as the metal film thickness is reduced [2]. Use of thicker metal films, as in the Otto scheme, allows reaching optical properties of the active layer close to those of the bulk. Furthermore, with the Otto configuration it is possible to use opaque substrates for the active layer, something not possible with the Kretschmann configuration. Use of CMOS compatible silicon substrates, for example, would bring all the processing benefits available in the integrated circuits industry, to allow integrating microfluidic as well as microelectronic circuitry, to the same substrate of the SPR supporting active layer, thus enabling development of new sensor architectures. Finally, by use of the Otto configuration one can fabricate devices with very thin channel heights — approximately two wavelengths for critical coupling of the SPR effect — in turn enabling

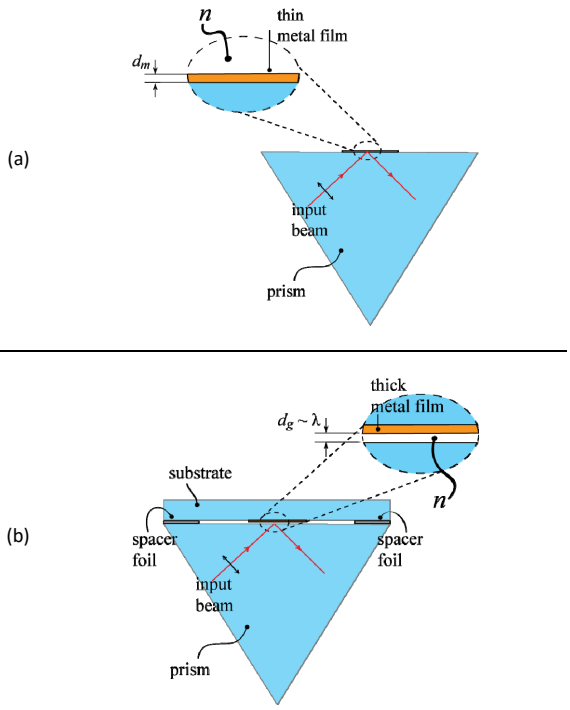


Fig.1. (a) Kretschmann and (b) Otto configurations for observation of the SPR effect on a metal surface in contact with a medium having refractive index *n*. In the Kretschmann configuration a thin metal film of thickness $d_m$ is employed and in the Otto configuration, the metal and the glass surfaces are separated by a gap distance $d_g$.

probing much smaller sample volumes, something that with the Kretschmann configuration could only be done at the expense of lowering the quality factor of the resonance effect.

The potential benefits of the Otto configuration for SPR-based optical sensing is the main motivation for developing the work described in the following sections, in which we report on the fabrication and characterization of a sealed Otto chip device capable of exhibiting the SPR effect.

## 2. Fabrication of the Otto Chip

In order to determine design parameters for the successful observation of the SPR effect in the Otto configuration, one has to assume known the optical constants of the metal so as to determine the gap distance that satisfy a given coupling condition. In this work gold was chosen as the metal and devices were projected to exhibit critical coupling for the SPR effect at a wavelength of 975.1 nm. The optical constants of gold were interpolated from those listed in the tables of the CRC Handbook of Chemistry and Physics [14]. All simulations reported in this paper were obtained by use of a *Mathematica* code that calculates the reflectance of a multilayer structure [15], employing the Fresnel reflection formulation reported in the literature [1,2,5] for a BK7 prism and for the wavelength of 975.1 nm, used in the experimental set-up reported herein. The refractive index of BK7 was obtained from [16] and the gap is assumed to be air or vacuum. Figure 2 shows the predicted SPR curves for the Otto configuration having the gap thickness as a parameter. As can be observed from the plots, for the chosen optical constants the projected gap thickness for critical coupling is approximately 2.12 μm.

For fabrication of the Otto chip device, a silicon wafer was used as substrate to fabricate four devices. First, an initial cavity with a depth of 2.5 μm was formed on the silicon substrate using a deep reactive ion etching (DRIE) process [17], with a thin positive photoresist (PR) used as an etch mask, as illustrated in Fig.3. Then, the PR was removed using an oxygen plasma etcher. A Cr film of 10 nm was sputtered on the silicon surface, followed by 300 nm of Au. After metal deposition, the metal coating was patterned inside the silicon cavity using the lift-off

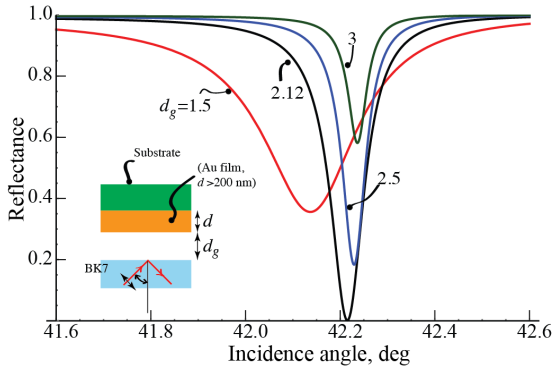


Fig.2. Dependence of the SPR effect on the gap thickness (in microns), for the Otto configuration.

process, by use of AZ5214 as a PR mold [18]. The backside of the silicon wafer was etched by use of a Bosch DRIE process [17], to yield the inlet and outlet of the channel of the chip, with aluminum used as the etch mask. The prepared silicon wafer along with a bare fused quartz wafer were diced with the same size, the latter used for sealing the channel as well as to serve as the input optical window of the chip.

Measurement of the etched channel depth and of the Cr/Au film thickness was done by use of two equipment, namely a mechanical profilometer — Alpha Step, Model ®500 — and a 2D laser profiler — KEYENCE, Model VF-7500, which allowed determining the ~ 2.20 μm gap between the top Si surface and the top metal surface, indicated in Fig.3f, with an error margin less than 2%.

Bonding of the silicon to the quartz surface is the most critical step in fabricating the chip, as care has to be taken to avoid offsetting the metal–glass gap distance. Anodic bonding is an effective way to achieve a perfect sealing between glass and silicon [19]. Usually in this process, a voltage of 800 V is applied between silicon and glass at a temperature of 400 °C for perfect sealing. However, our device has a very large area of the gold surface with a very small gap — ~2.2 μm — between the glass and the silicon substrate. Thus, a very high electric field is formed between silicon and gold, in turn leading to field emission that ends up damaging the gold layer [20]. As a result, the gold surface becomes black and both its roughness and resistivity increase substantially. Because of this the high voltage application step should be avoided in the sealing process.

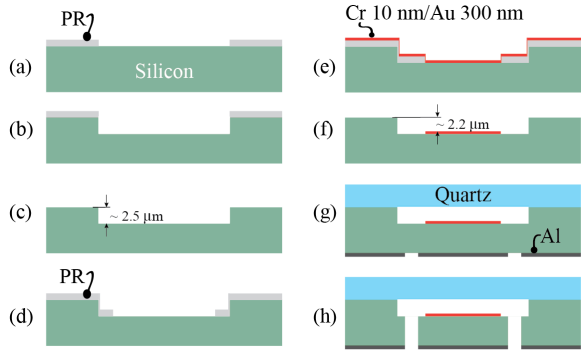


Fig.3. (a) PR is patterned on Si substrate. (b) A 2.5 μm cavity is produced by DRIE and (c) PR is removed. (d) Positive PR added. (e) Metallization and (f) PR removal. (g) Quartz plate is bonded and (h) channels are etched through Al mask.

Oxygen plasma-assisted bonding process for silicon/quartz bonding does not need a high–voltage application and it was employed in place of the anodic bonding process. The silicon substrate was bonded with the fused quartz sample after RCA1 cleaning and oxygen RIE process [21]. After manual bonding, the initial bonded wafer is annealed on a hotplate at 200 °C during 2 hours. Originally, an oxygen plasma-assisted silicon/quartz wafer level bonding makes a permanent bonding, but chip (sample) level bonding sometimes shows poor bonding quality due to small bonding area [22]. A lateral external force

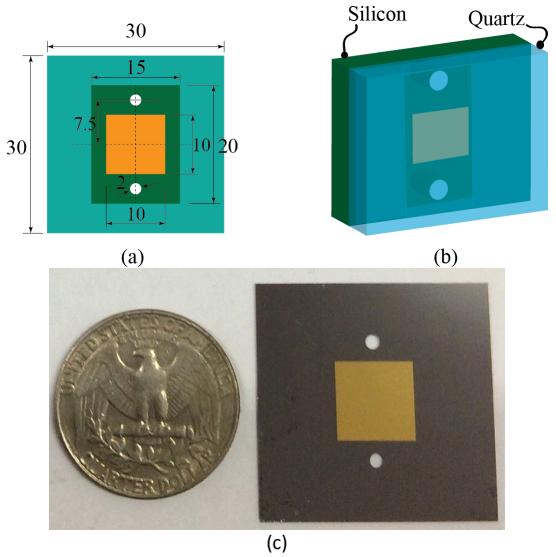


Fig.4. (a) Top view of the Otto chip (all dimensions in mm). (b) 3D illustration of the Otto chip. (c) Picture of the Otto chip.

was applied to the chip and no noticeable damage or detachment was observed and it was thus confirmed that the bonding strength was enough to run the first experiments. Figure 4a shows a top view and Fig.4b illustrates the appearance of the Otto chip device. Figure 4c shows a picture illustrating the relative size of the chip measured in this work.

## 3. Measurement of the SPR Effect on the Otto Chip

Measurement of the Otto chip response was made by use of an automated reflectometer operating at a wavelength of 975.1 nm [23]. A simplified representation of the measurement system is shown in Fig.5. A right angle BK7 coupling prism is used to observe the SPR effect, with the chip placed in optical contact with the prism's top surface, as shown in the figure. The output laser beam is transmitted through an iris — not shown in Fig.5 — which reduces the beam diameter to approximately 1 mm. The laser beam polarization is set parallel to the incidence plane by use of the polarizer *P*. Part of the input beam is reflected by the splitter *S* and detected by the reference photodetector $D_R$. The transmitted beam after reflection on the prism top surface is detected by the photodetector $D_S$. The signals of $D_R$ and $D_S$ are sent to two channels of a DAS-16 data acquisition board (Keythley-Metrabyte) slotted on a PC for processing.

One important feature in measuring the SPR effect in the near infrared is that in this spectral region the effect is expected to occur within a very narrow angular range, as can be inferred from Fig.2. Therefore angular and positioning controls of the sample have to be highly precise. In the arrangement of Fig.5, computer controlled translation movements are provided by step motors, corresponding to two orthogonal directions along the prism top surface and one orthogonal to it, for beam footprint positioning, along with rotation of the prism as well as positioning of the signal photodetector, that tracks the reflected beam direction. By doing this it is possible to sweep the incidence angle across 12 degrees, with a resolution of 0.005 degrees. In addition, the system has a built-in translation compensation algorithm [24] to correct for the refraction in the input face of the prism during angular scan of the rotation stage. This algorithm ensures that the laser footprint on the sample remains stationary regardless of the laser beam incidence angle.

Figure 6 shows the experimental SPR curve measured on one of the fabricated Otto chips. As can be noticed, the SPR effect is present but it does not exhibit maximum absorption on resonance, as originally predicted from the Fresnel reflection formulation obtained with use of the Au optical constants listed in [14]. One possible source of discrepancy of the measured resonance relative to that predicted theoretically could be the existence of surface roughness [4]. Figure 7

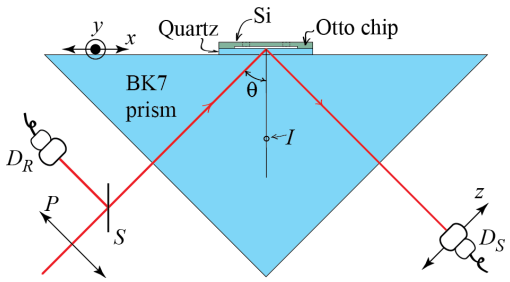


Fig.5. Simplified scheme of the automated reflectometer used to characterize the SPR response of the Otto chip.

shows an AFM picture of a 5 μm² portion of the Au surface, prior to sealing with the quartz plate. The rms —root-mean-square — roughness was measured along the black horizontal line shown in the picture and a value of 2.9 nm was obtained. This value is too small to yield any appreciable change in the dispersion relation of surface plasmons relative to that expected from a smooth surface, in the infrared spectral region [4].

A nonlinear regression analysis algorithm was written in *Mathematica*, with use of the built–in function *FindFit*, to adjust the refractive index *n*, extinction coefficient κ and gap thickness $d_g$ of the Otto chip from the model to the data. Two sets of best-fit parameters were obtained, yielding the solid curves that are undistinguishable in the plot of Fig.6. The existence of two sets of solutions from nonlinear regression analysis of SPR data was pointed out previously by Chen and Chen [5] and is very likely to occur when the SPR curve exhibits a symmetrical, lorentizan–type lineshape, which is the case for a gold surface in the near infrared. The two solutions are listed in Table I. Taking into account the gap thickness of 2.2 μm measured with the optical profilometer of the Otto chip, prior to sealing, solution 2 of

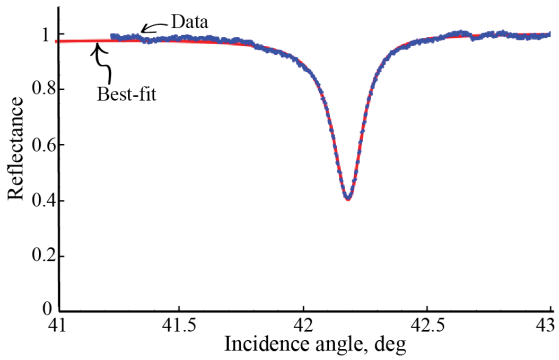


Fig.6. Data and best-fit for the solutions listed in Table I.

Table I was chosen to represent the measured data.

It is important to notice that there is a wide range of values of optical constants measured and reported in the literature, as pointed out by Boreman *et al* [25] and the choice of one or other listed value has direct influence on the projected gap thickness for critical coupling in the Otto configuration. This influence appears in the gap thicknesses calculated at critical coupling for the distinct optical constants listed in Table II. As no previous data was available for the gold films produced in our sputtering apparatus, we chose to use the optical constants from [14] to estimate the gap thickness. Thus, by use of the solution set 2 of Table I for the complex refractive index of the gold surface, the predicted gap thickness for critical coupling is 1.67 μm for the type of gold film sputtered in our apparatus, as listed in the last line of Table II.

It is important to point out that even though a critical coupling condition was not obtained in the fabricated device, the calculated sensitivity — maximum change in reflectance to an incremental change in refractive index of the air gap — was the same as that at critical coupling. The calculated sensitivity is approximately 300 either for the parameters in the second line of Table I or for those in the last

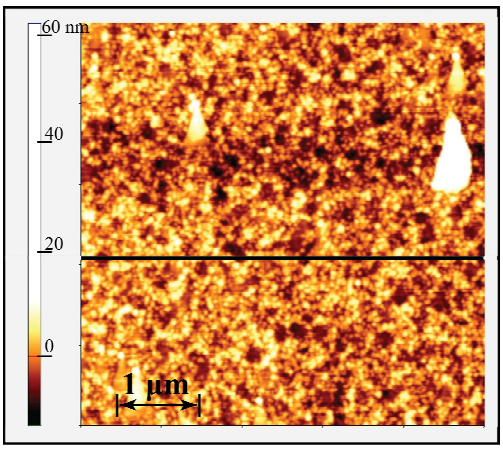


Fig. 7. AFM picture of the Au surface of the Otto chip prior to sealing. The black horizontal line corresponding to the cut through which the rms roughness was determined.

line of Table II. Regarding dynamic range, one can notice from Fig.6 that the fabricated device has a maximum resonance depth which is 60% of that at critical coupling, a not too significant reduction for sensing applications.

## 4. Conclusions

It is expected that the Otto chip device might find important new applications both for biosensing and gas sensing. In biosensing, for example, further miniaturized reactor configurations in which the functionalized dextran layer [11], typically used in SPR-based biointeraction analysis devices, fills up the entire flow channel can be used. Use of very narrow flow channels, as in the Otto chip, will allow observation of real time interactions without diffusion time limitations due to dead volumes in the flow channel, given that the carrier solution having the analyte has to flow through the sensitive layer that fills up the entire channel. For gas sensing, use of gas sensitive layers underneath the gold film, which swell when exposed to specific gases can lead to new, highly sensitive devices. Future work on the Otto chip will be directed to fabricating additional devices with the predicted gap thickness corresponding to the best-fit shown in Table II, as well as to determining the reproducibility of the SPR effect amongst different devices, including a more in–depth study of the sealing capability of the bonding technique used to seal the chip.

## Funding Information

Conselho Nacional de Desenvolvimento Científico e Tecnológico (CNPq – Brazil) (56066520105); NRF–Korea (NRF–2013K2A1A2049144), MINECO–Spain (PIB2010BZ-00585); GENCAT–Spain (2014 SGR 1551).

**Table I - Best fit results from the regression analysis.**

| Solution set | n | $\kappa$ | $d_g$, µm |
|---|---|---|---|
| 1 | 0.05 | 6.08 | 1.67 |
| 2 | 0.27 | 6.27 | 2.35 |

**Table II - Predicted gap thicknesses for critical coupling for different data on the optical constants of gold.**

| Reference | $n$ | $\kappa$ | $d_g$, µm |
|---|---|---|---|
| 14 | 0.09 | 6.11 | 2.12 |
| 25 | 0.15 | 6.41 | 1.96 |
| 26 | 0.22 | 6.28 | 1.76 |
| Best-fit | 0.27 | 6.27 | 1.67 |

## References

1. A. Otto," Excitation of Nonradiative Surface Plasma Waves in Silver by the Method of Frustrated Total Reflection," Z. Physik **216**, 398-410 (1968).
2. E. Kretschmann, "Determination of optical constants of metals through the stimulation for surface plasma oscillations," (in German), Z. Physik **241**, 313-324 (1971).
3. R. W. Wood, "On a remarkable case of uneven distribution of light in a diffraction grating spectrum," Proceedings of the Physical Society of London **18,** 269-275 (1902).
4. E. Fontana and R. H. Pantell, "Characterization of multilayer rough surfaces by use of surface-plasmon spectroscopy," Physical Review **B 37**, 3164–3181 (1988).
5. W. P. Chen and J. M. Chen, "Use of surface plasma waves for determination of the thickness and optical constants of thin metallic films," Journal of the Optical Society of America **71**, 189-191 (1981).
6. M. Moskovits, "Surface-enhanced spectroscopy," Reviews of Modern Physics **57,** 783-826 (1985).
7. B. Liedberg, C. Nylander and I. Lundstrom, "Surface plasmon resonance for gas detection and biosensing," Sensors and Actuators **4**, 299-304 (1983).
8. M. T. Flanagan and R. H. Pantell, "Surface plasmon resonance and immunosensors," Electronics Letters **20**, 968–970 (1984).
9. E. Fontana, R. H. Pantell and S. Strober, "Surface plasmon immunoassay," Applied Optics **29**, 4694-4704 (1990).
10. S. Sjolander and C. Urbanicczky, "Integrated fluid handling system for biomolecular interaction analysis," Analytical Chemistry **63**, 2336-2345 (1991).
11. B. Liedberg, I. Lundstrom and E. Stenberg, "Principles of biosensing with an extended coupling matrix and surface plasmon resonance," Sensors and Actuators **B 11**, 63-72 (1993).
12. E. Fontana, R. H. Pantell and M. Moslehi, "Characterization of dielectric-coated, metal mirrors using surface plasmon spectroscopy," Applied Optics **27**, 3334-3340 (1988).
13. E. K. Akowuah, T. Gorman, and S. Haxha, " Design and optimization of a novel surface plasmon resonance biosensor based on Otto configuration," Optics Express **17**, 23511-23521 (2009).
14. D. R. Lide, ed., Handbook of Chemistry and Physics, 85th ed.(CRC, 2005), pp. 12.133 –12.156.
15. E. Fontana, "Multilayer reflectance," pp. 1–4, http://goo.gl/Hm6DA3, Accessed February 21, 2015.
16. M. Bass, ed., Handbook of Optics, 2nd ed. (McGraw-Hill, 1995), Vol. II, Ch. 33, pp. 33.3–33.101.
17. Y. S. Lee, Y. H. Jang, Y. K. Kim, and J. M. Kim, "Thermal de–isolation of silicon microstructures in a plasma etching environment," Journal of Micromechanics and Microengineering, Vol.23, No. 2, 025026 (2013).
18. H. W. Park, Y. K. Kim, H. G. Jeong, J. W. Song, and J. M. Kim, "Feed-through capacitance reduction for a micro–resonator with push–pull configuration based on electrical characteristic analysis of resonator with direct drive," Sensors and Actuators A, Vol. 170, No. 1, pp. 131–138 (2011).
19. H. Henmi, S. Shoji, Y. Shoji, K. Yoshimi and M. Esashi, "Vacuum packaging for microsensors by glass-silicon anodic bonding," Sensors and Actuators A, Vol. 43, No. 1, pp. 243–248 (1994).
20. A. J. Wallash, L. Levit, "Electrical breakdown and ESD phenomena for devices with nanometer-to-micron gaps," Proceedings of SPIE, Vol. 4980, pp. 87–96 (2003).
21. T. Suga, T. H. Kim, and M. M. R. Howlader, "Combined process for wafer direct bonding by means of the surface activation method," Proceeding of the 54th. IEEE Electronic Components and Technology Conference, pp. 484–490 (2004).
22. R. Stengl, T. Tan, U. Gösele, "A Model for the silicon wafer bonding process," Japanese Journal of Applied Physics, Vol. 28, No. 10, pp. 1735-1741 (1989).

23. G. O. Cavalcanti, M. A. Luna and E. Fontana, "Automated reflectometer for surface plasmon resonance studies in the infrared and its application for the characterization of Pd films," Proceedings of the SBMO/IEEE MTT-S International Microwave and Optoelectronics Conference, pp. 688–701 (2007).
24. E. Fontana and G. O. Cavalcanti, "Maintaining a stationary laser footprint during angular scan in internal reflection experiments," Applied Optics, Vol. 52, No. 32, pp. 7669–7674 (2013).
25. Glenn D. Boreman, Timothy Johnson, Andrew C. Jones, Sang-Hyun Oh, Robert L. Olmon, Markus B. Raschke, David Shelton, and Brian Slovick, "Broadband Electrical Permittivity of Gold for Plasmonics and Nano-Optics Applications," 2011 Conference on Lasers and Electro-Optics (CLEO 2011), pp.1–2.
26. P. B. Johnson and R. W. Christy, "Optical constants of the noble metals," Physical Review B, Vol. 6, No. 12, pp. 4370-4379 (1972).